Supporting Information

Identification of Stable Species Formed under CO Adsorption and Oxidation on Alumina-supported Single Pt Atoms: Why Nanoparticles are More Active

Franck Morfin,[1] Caroline Dessal,[1] Alexis Sangnier,[2] Céline Chizallet,[2,*] Laurent Piccolo[1,*]

[1] *IRCELYON, CNRS & Université Lyon 1, 69100 Villeurbanne, France*

[2] *IFP Energies nouvelles, Rond-point de l'échangeur de Solaize, BP3, 69360 Solaize, France*

* Corresponding authors: Laurent.Piccolo@ircelyon.univ-lyon1.fr; Celine.Chizallet@ifpen.fr

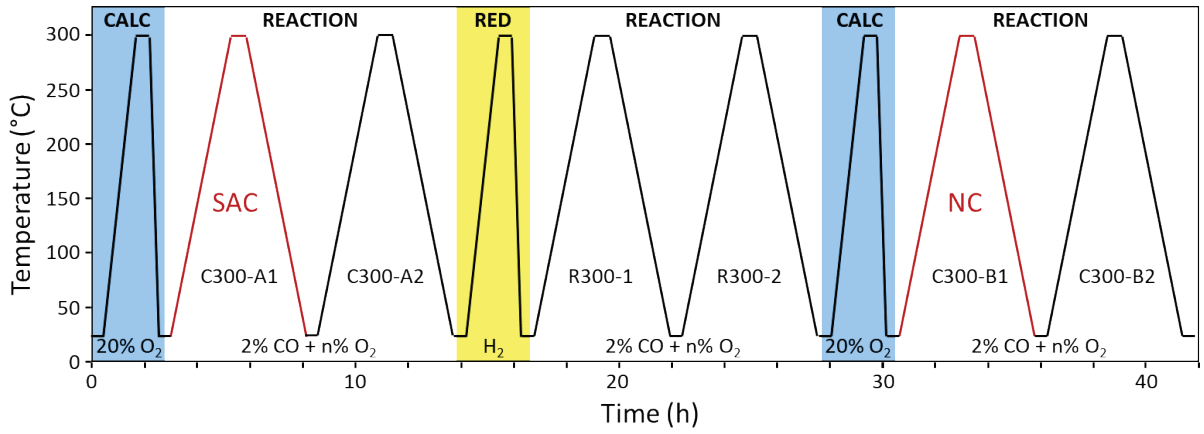

Figure S1. Protocol of DRIFTS-MS-monitored CO oxidation experiments on Pt/Al_2O_3 catalysts. CALC and RED correspond to calcination and reduction steps, respectively. The n value is 2 or 10, depending on the chosen conditions. The cycles in red correspond to the steps selected for the comparison of the single-atom catalyst (SAC) and the nanocatalyst (NC). In the following Figures S3-S10 containing the whole set of DRIFTS data, the reaction cycles are denoted C300-A1, C300-A2, R300-1, R300-2, C300-B1, and C300-B2. For CO desorption experiments, after calcination or reduction, 2% CO in He was flowed at RT for 20 min, the cell was purged with He flow at RT for 20 min, and one temperature cycle under pure He flow was performed.

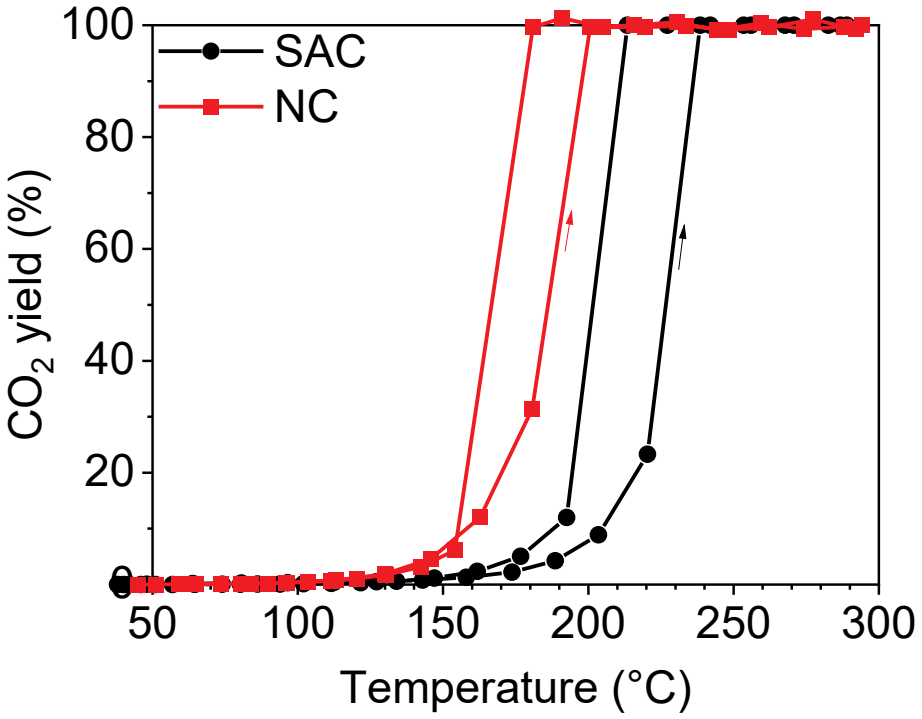

Figure S2. CO_2 yield versus temperature on pre-calcined 0.3 wt% Pt/γ-Al_2O_3 (SAC) and pre-reduced 1 wt% Pt/γ-Al_2O_3 (NC) catalysts under $CO:O_2$=2:10% reaction conditions. The same quantity of Pt (500 μg) was used in both cases. Heating/cooling ramp rates: 1 °C/min. Total flow rate: 50 mL/min. Data extracted from Ref. 1.

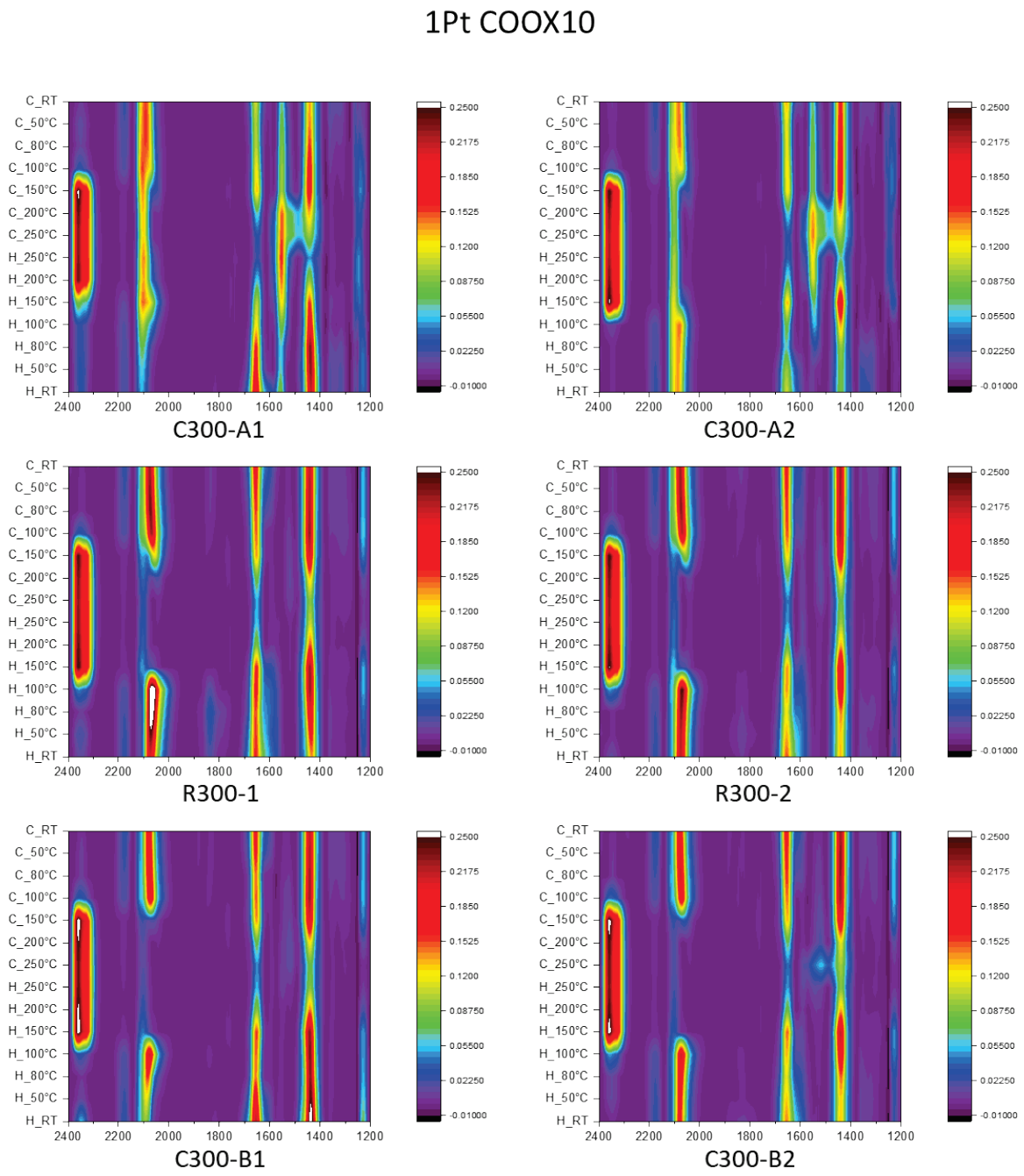

Figure S3. DRIFTS experiments on 1 wt% Pt/γ-Al_2O_3 under CO:O_2=2:10% reaction conditions. X axis corresponds to wavenumbers in cm^{-1}. On Y axis, H and C denote heating and cooling steps, respectively. The data at 300 °C (maximum temperature) were removed because of wrong signal due thermally-induced beam dealignment.

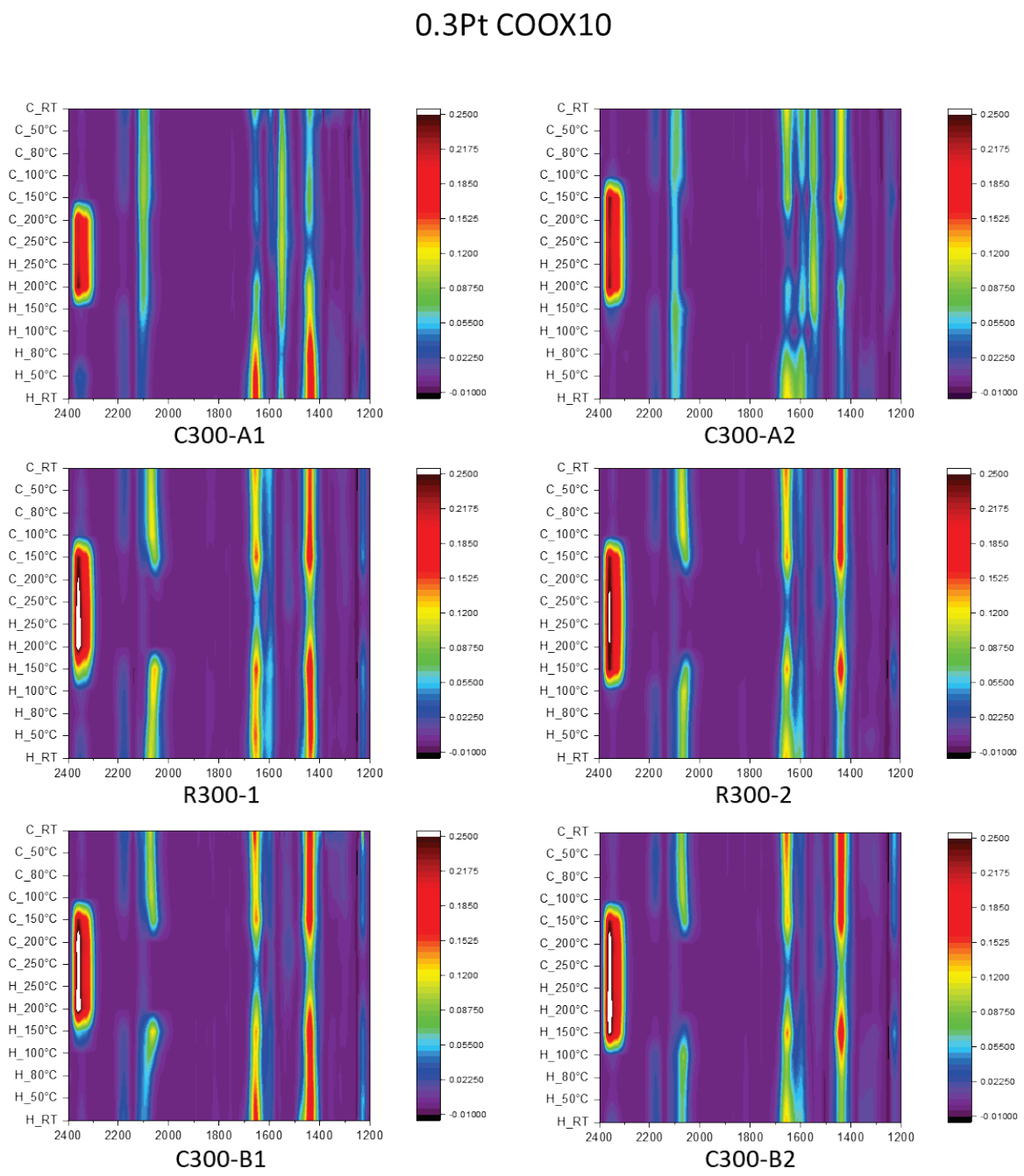

Figure S4. DRIFTS experiments on 0.3 wt% Pt/γ-Al_2O_3 under CO:O_2=2:10% reaction conditions. X axis corresponds to wavenumbers in cm^{-1}. On Y axis, H and C denote heating and cooling steps, respectively. The data at 300 °C (maximum temperature) were removed because of wrong signal due thermally-induced beam dealignment.

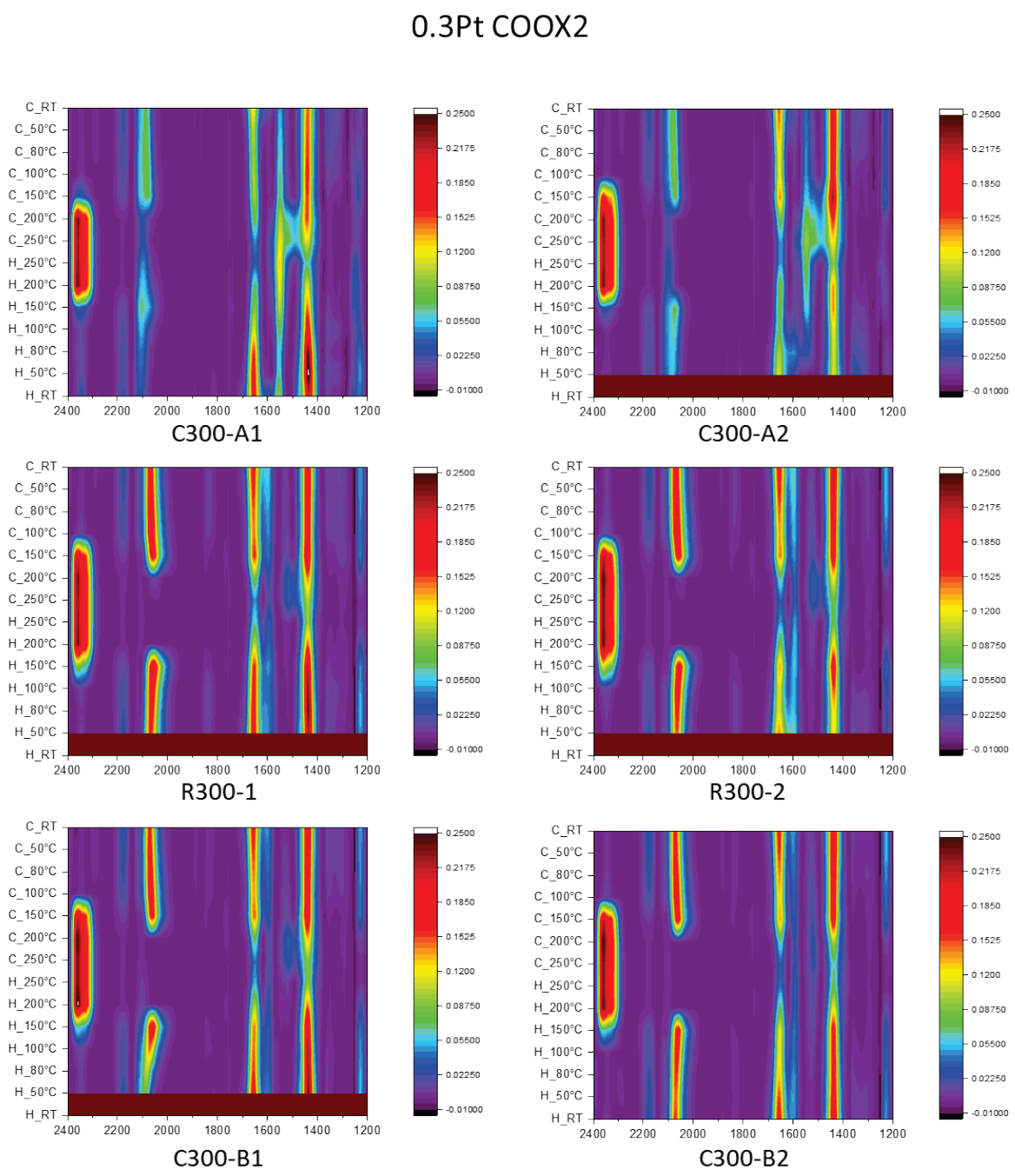

Figure S5. DRIFTS experiments on 0.3 wt% Pt/γ-Al_2O_3 under CO:O_2=2:2% reaction conditions. X axis corresponds to wavenumbers in cm^{-1}. On Y axis, H and C denote heating and cooling steps, respectively. The data at 300 °C (maximum temperature) were removed because of wrong signal due thermally-induced beam dealignment.

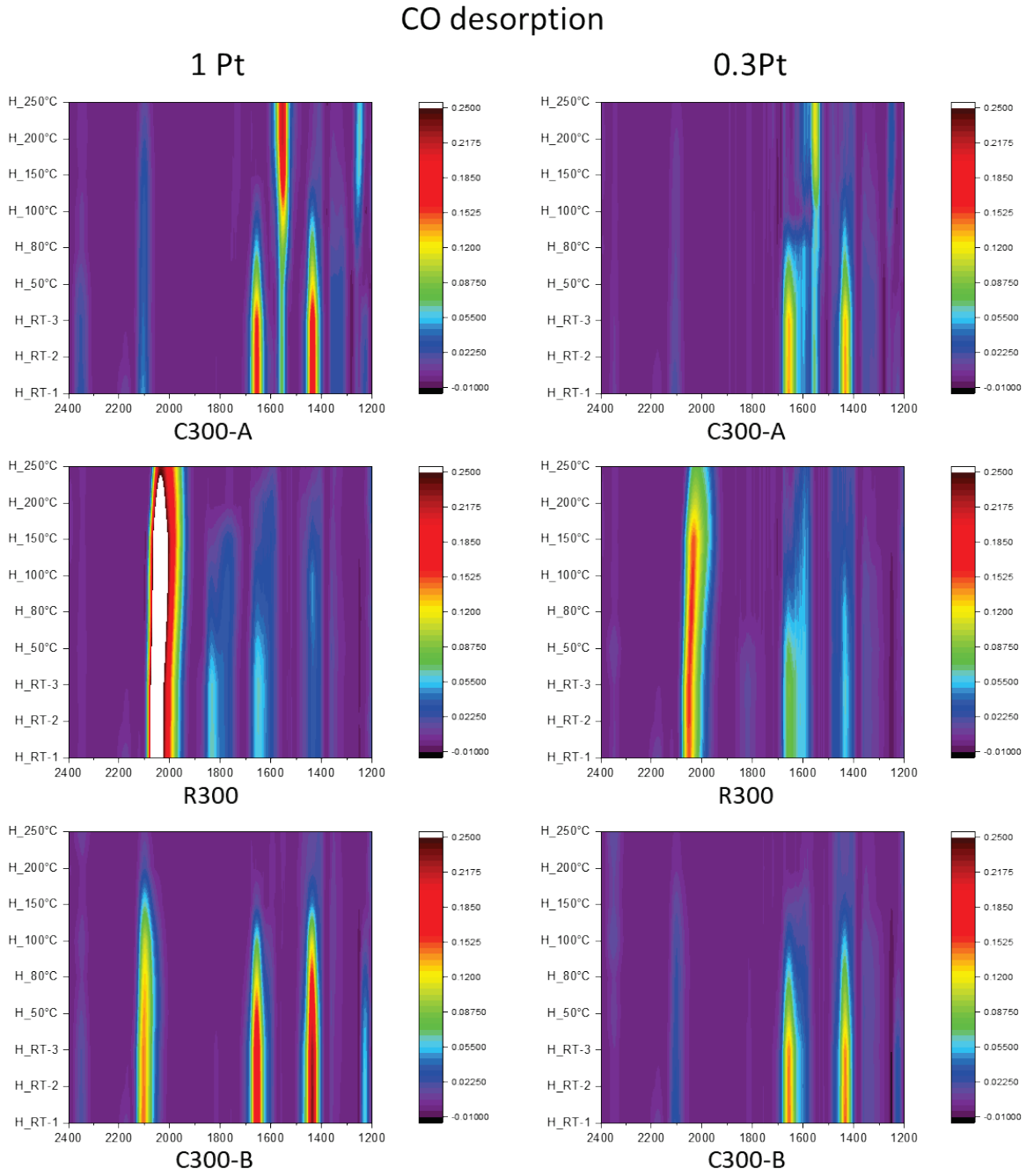

Figure S6. CO desorption DRIFTS experiments on 1 wt% (left panel) and 0.3 wt% (right panel) Pt/γ-Al_2O_3. X axis corresponds to wavenumbers in cm^{-1}. On Y axis, H and C denote heating and cooling steps, respectively. The data at 300 °C (maximum temperature) were removed because of wrong signal due thermally-induced beam dealignment.

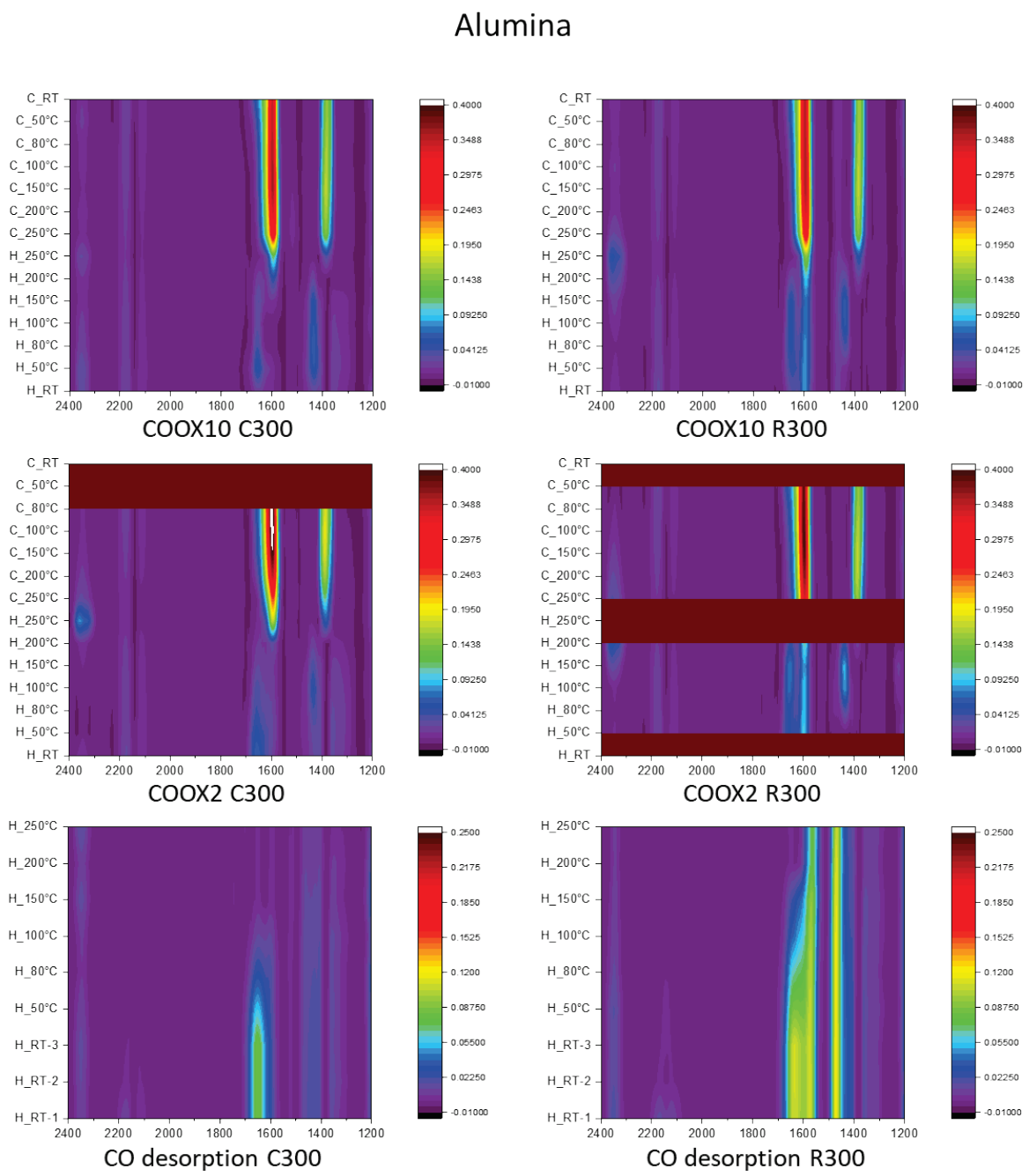

Figure S7. DRIFTS experiments on γ-Al_2O_3 under CO:O_2=2:10% reaction (top row), CO:O_2=2:2% (middle row), and CO desorption (bottom row) conditions. X axis corresponds to wavenumbers in cm^{-1}. On Y axis, H and C denote heating and cooling steps, respectively. The data at 300 °C (maximum temperature) were removed because of wrong signal due thermally-induced beam dealignment.

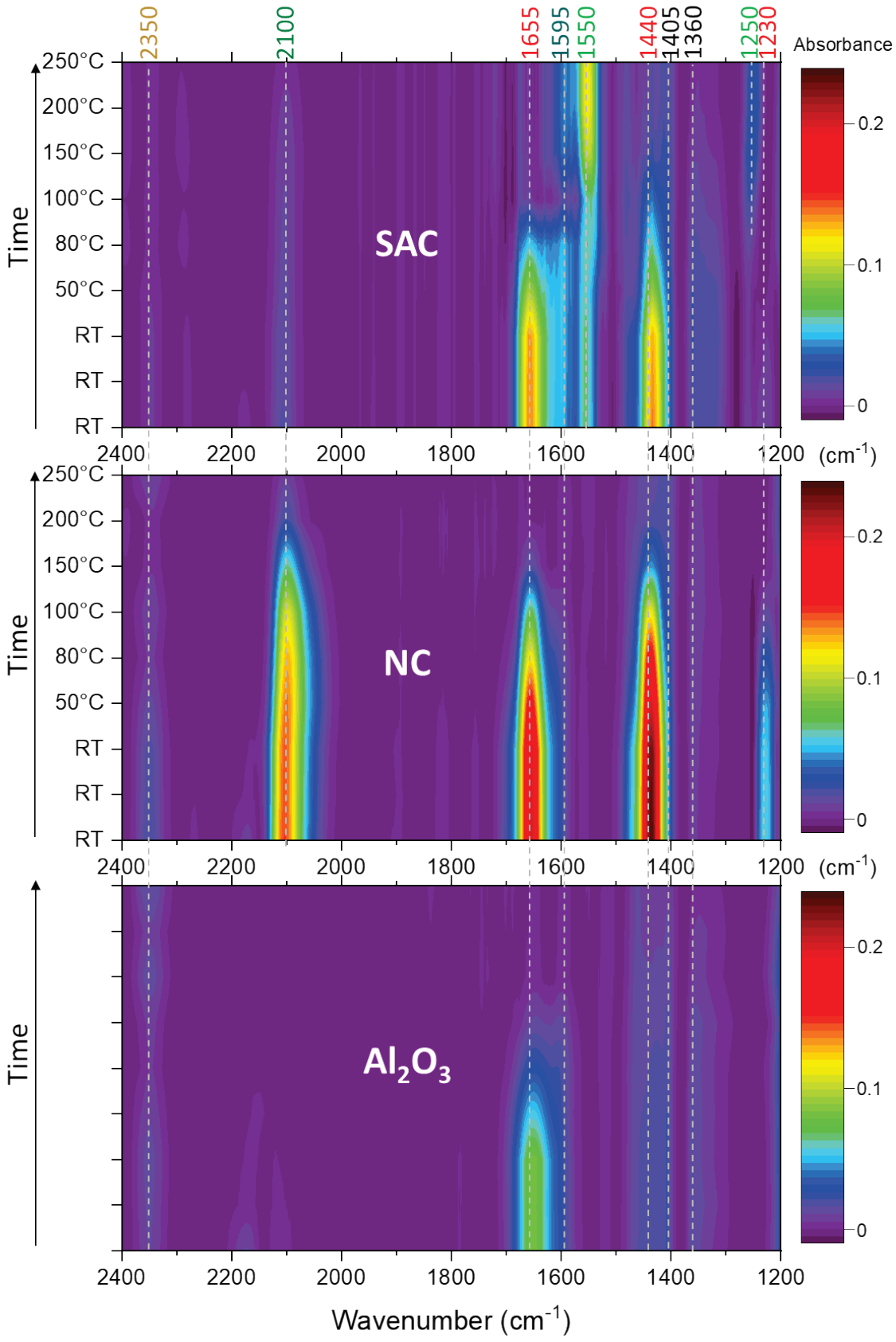

Figure S8. Comparison of CO desorption DRIFTS experiments on 0.3 wt% Pt/γ-Al_2O_3 (C300-A1 cycle), 1 wt% Pt/γ-Al_2O_3 (C300-B1 cycle), and γ-Al_2O_3 (C300 cycle).

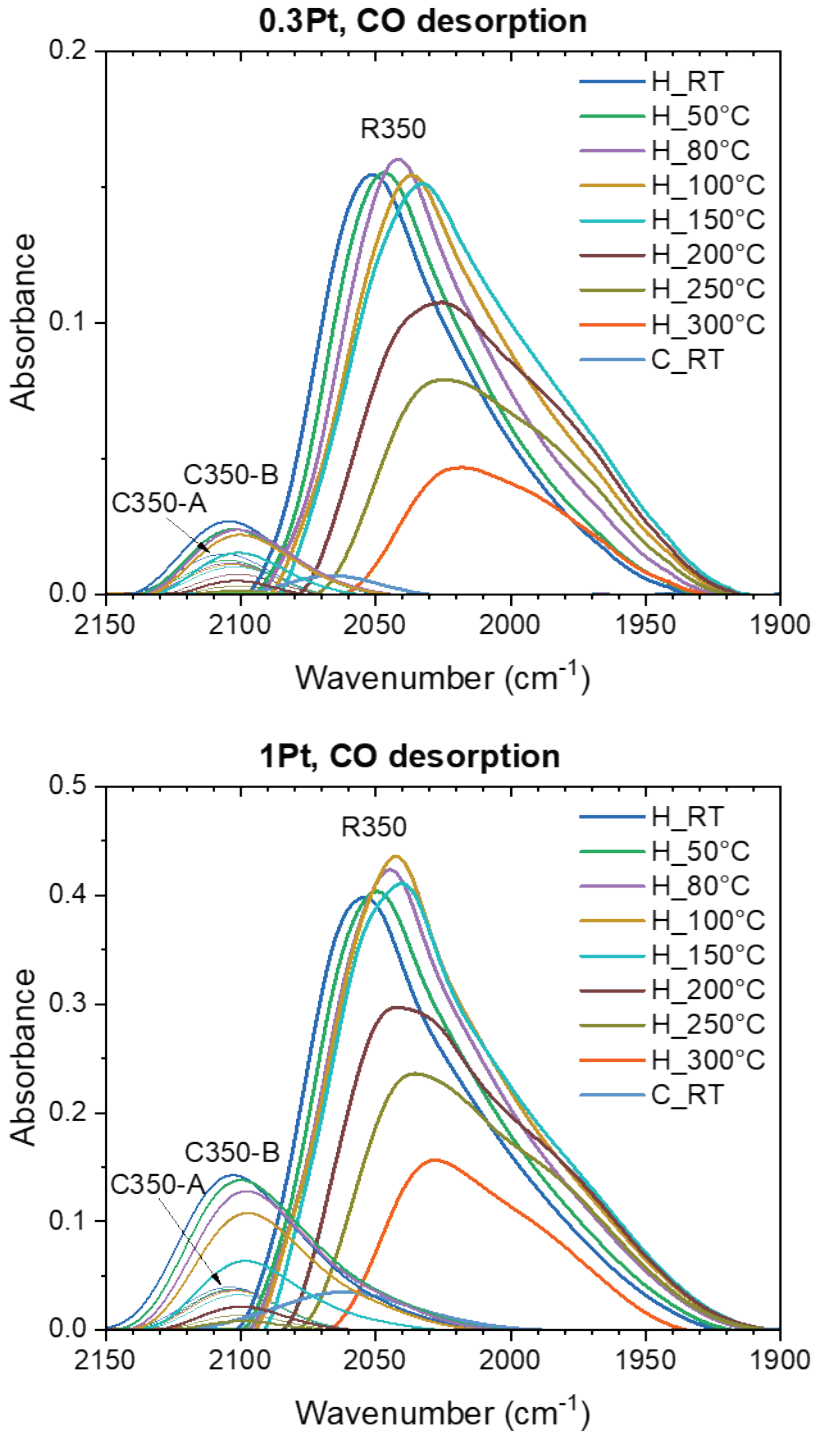

Figure S9. CO desorption DRIFTS spectra (C-O stretching region) on 0.3 wt% Pt/γ-Al_2O_3 and 1 wt% Pt/γ-Al_2O_3. H and C stand for heating and cooling steps.

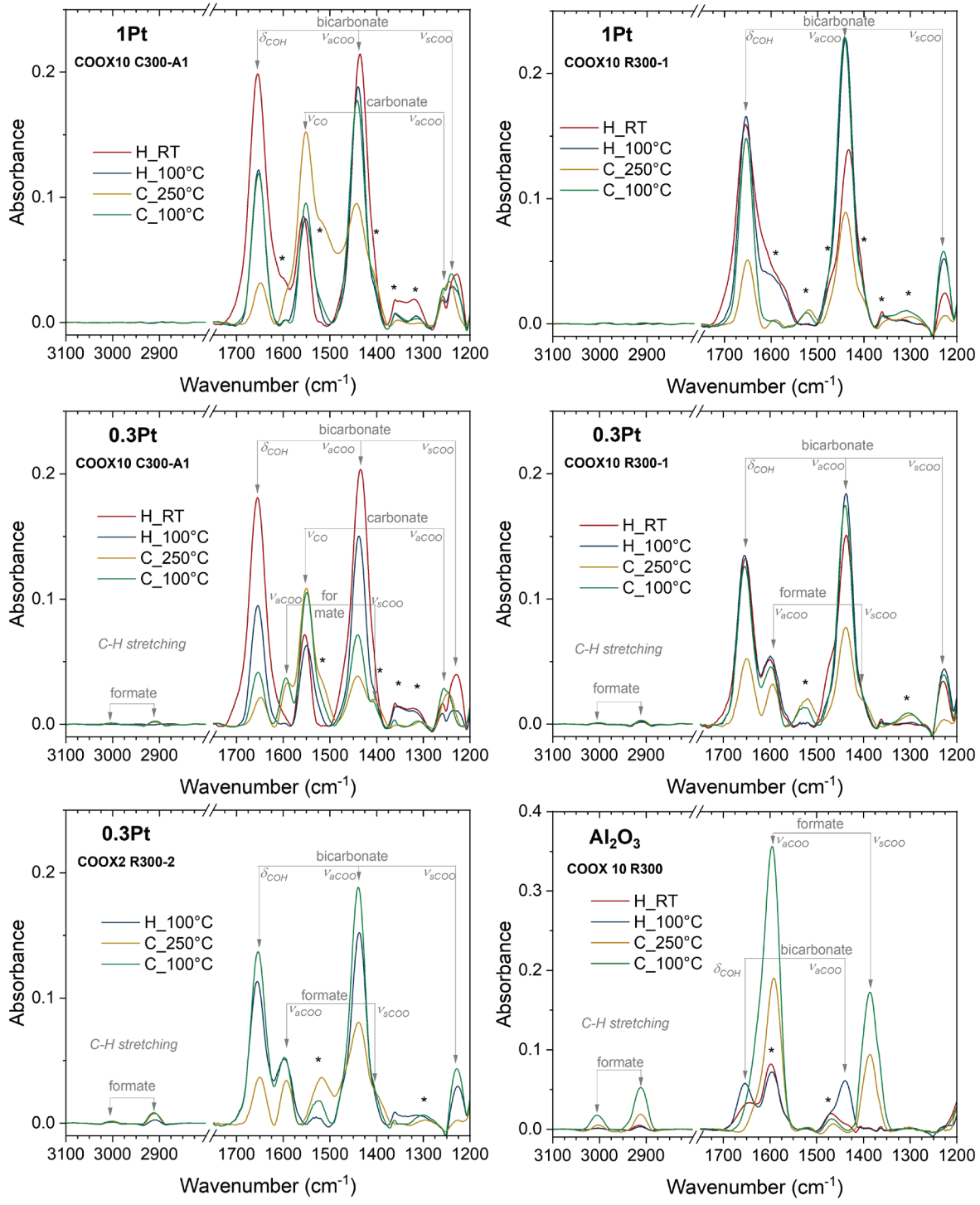

*Figure S10. Identification of formate species through correlation between C-H stretching (left panel) and COO stretching (right panel) DRIFTS features: they appear clearly on alumina, weakly on 0.3Pt sample, not on 1Pt sample. Bicarbonates (all samples) and carbonates (pre-oxidized samples) are also visible. H and C stand for heating and cooling steps. * non-attributed bands.*

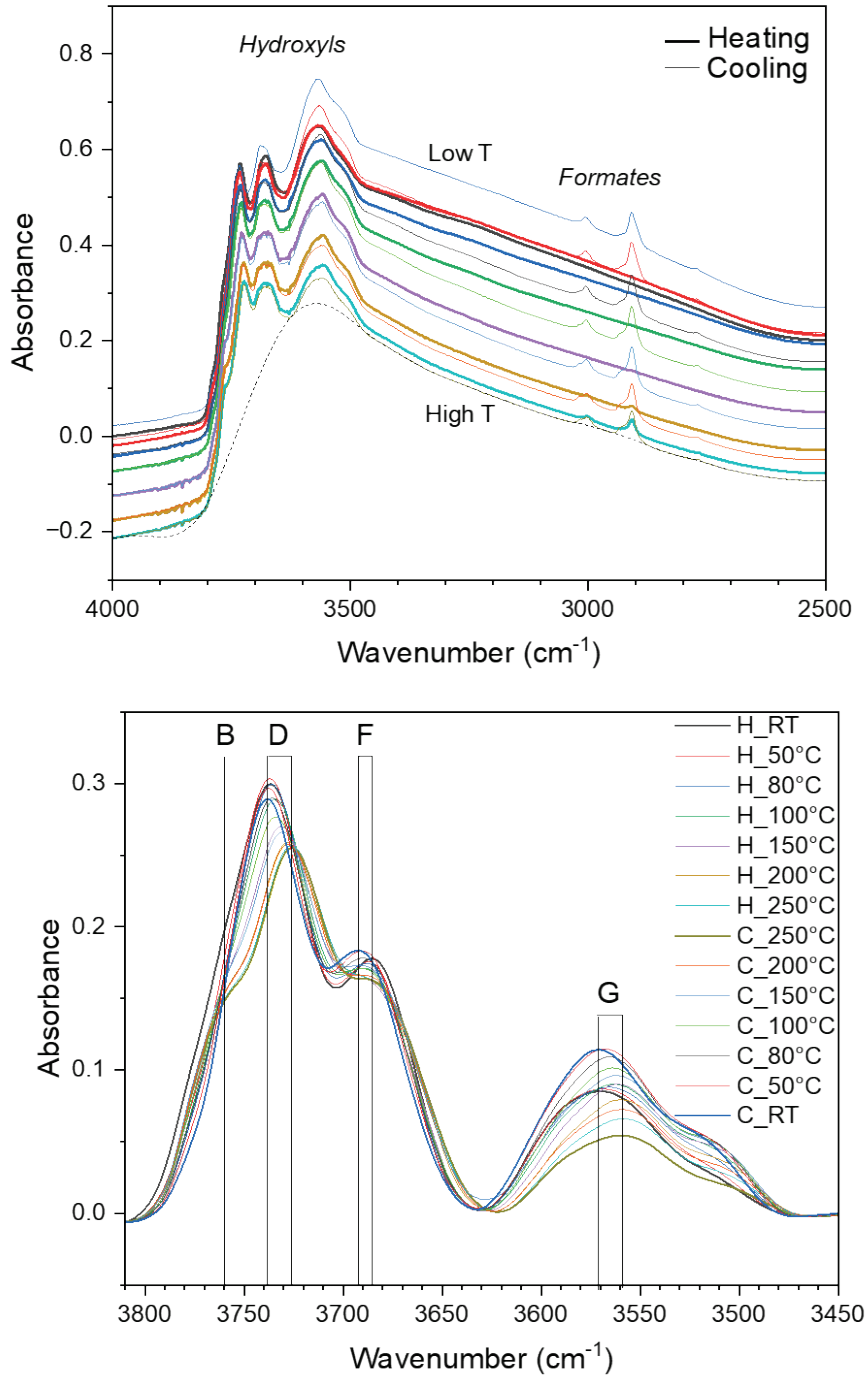

Figure S11. DRIFTS spectra (O-H stretching region) recorded for γ-Al_2O_3 under CO:O_2=2:10% conditions after calcination. Top: raw spectra. Bottom: spectra obtained by smoothing of raw spectra and subtracting a baseline (example: dotted line in top graph) to facilitate the comparison between hydroxyl bands. OH bands are labelled after Hadjiivanov.[2] The same colors are used for corresponding top and bottom graph spectra. H and C stand for heating and cooling steps.

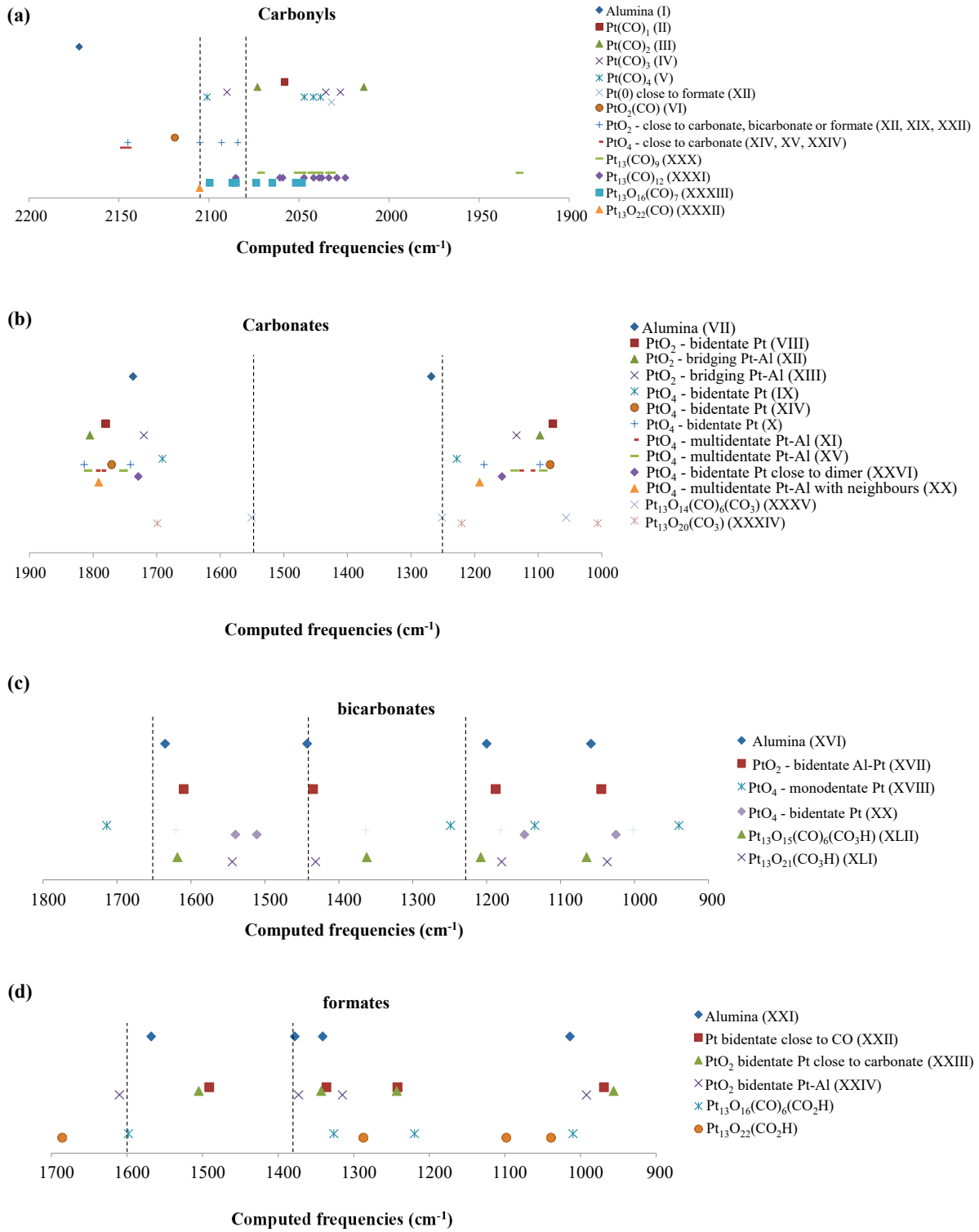

Figure S12. Distribution of the computed frequencies in the most relevant spectral zones addressed in the DRIFTS study for (a) carbonyls, (b) carbonates, (c) bicarbonates, and (d) formates. Vertical lines show the positions of the most relevant experimental bands.

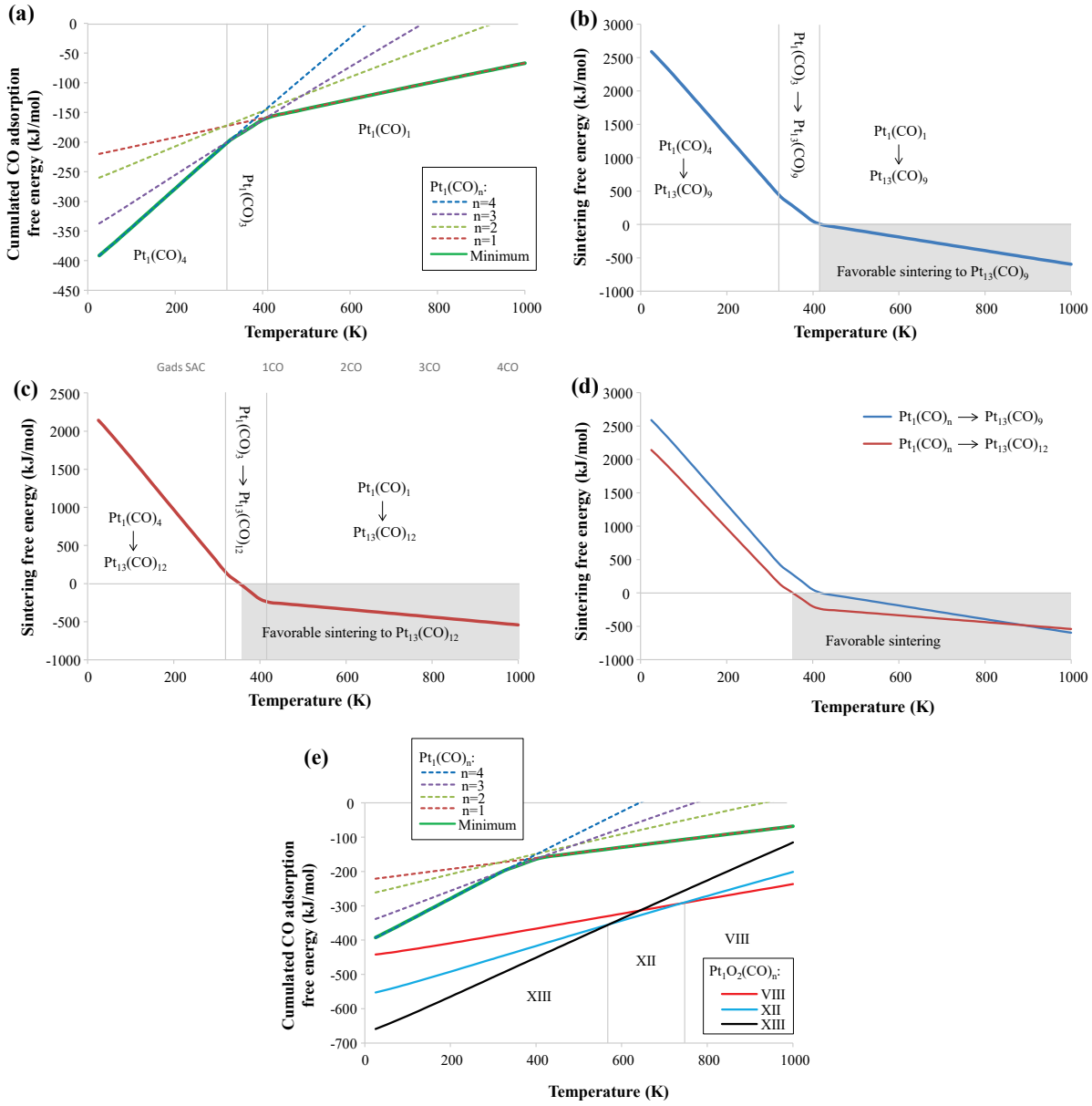

Figure S13. Computed thermodynamic diagrams at a CO partial pressure of 20 mbar for alumina-supported species. a) Cumulated adsorption free energy of CO for $Pt_1(CO)_n$ ($0 \leq n \leq 4$). b) Free energy of sintering from $Pt_1(CO)_n$ ($0 \leq n \leq 4$) to $Pt_{13}(CO)_9$. c) Free energy of sintering from $Pt_1(CO)_n$ ($0 \leq n \leq 4$) to $Pt_{13}(CO)_{12}$. d) Comparison of the free energy values depending on the final state, showing that sintering is more favorable when ending with $Pt_{13}(CO)_{12}$. e) Cumulated adsorption free energy of CO for $Pt_1(CO)_n$ (same as a) and $PtO_2(CO)_n$.

Table S1: Selection of experimental versus computed (harmonic, unscaled) wavenumbers for species containing carbonates as reported in the literature.

Species	**Modes**	**Experimental wavenumbers (cm^{-1})**	**Computed wavenumbers (cm^{-1})**	**Computational details**	**References exp./comput.**
Free carbonate	*E'* A_1' A_2'' *E'*	1415 1063 879 680	1452 1014 876 665	6-31G* B3LYP	[3]/[4]
CO_3/Pt(111)	A_1	1455 1537	1592 (long bridge) 1657 (short bridge)	Pt_{20} clusters 6-31G*, RECP (Pt) B3LYP	[5]/[4]
CO_3/Pt(111)	$\nu_{C=O}$ $\nu_{as(COO)}$	1457/1537 Not measured	1591/1686 1177/1140 (short/long bridge)	Periodic Plane waves (400 eV) PW91	[6]/[6]
CO_3/m-ZrO_2 (-111)	$\nu_{C=O}$ $\nu_{as(COO)}$	1524/1570 1350/1325	1667/1791 1239/1158 (tridentate/bidentate)	Periodic Plane waves (400 eV) PW91	[7]/[8]
(dppp)$PtCO_3$[a]	$\nu_{C=O}$	1661	1737	See Section 2.4	[9]/this work

[a] dppp is 1,3-bis(diphenylphosphino)propane. The (dppp)$PtCO_3$ complex is depicted below (color code: C grey, H white, O red, P purple, Pt blue):

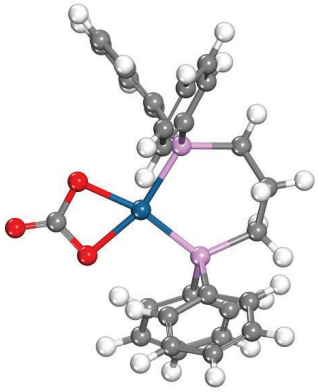

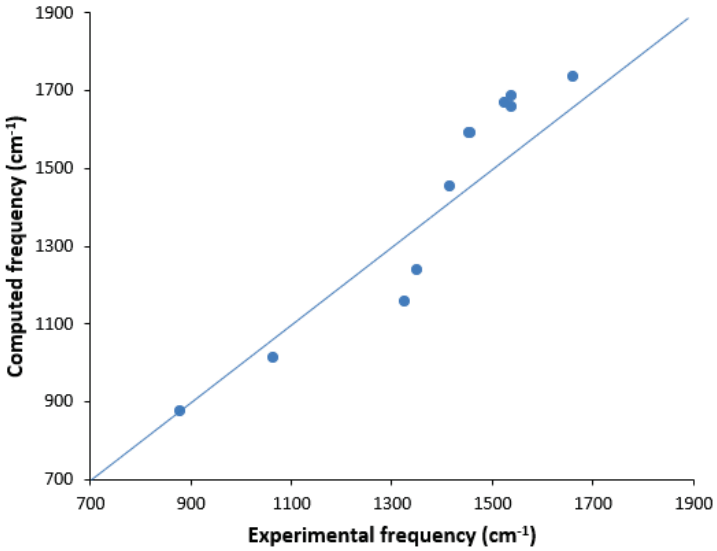

Figure S14. Computed vs. experimental values for carbonate vibration wavenumbers, extracted from Table S1. The straight line represents y=x function.

References

(1) Dessal, C.; Len, T.; Morfin, F.; Rousset, J.-L.; Aouine, M.; Afanasiev, P.; Piccolo, L. Dynamics of Single Pt Atoms on Alumina during CO Oxidation Monitored by Operando X-Ray and Infrared Spectroscopies. *ACS Catal.* **2019**, *9*, 5752–5759. https://doi.org/10.1021/acscatal.9b00903.

(2) Hadjiivanov, K. Chapter Two - Identification and Characterization of Surface Hydroxyl Groups by Infrared Spectroscopy. In *Advances in Catalysis*; Jentoft, F. C., Ed.; Academic Press, 2014; Vol. 57, pp 99–318. https://doi.org/10.1016/B978-0-12-800127-1.00002-3.

(3) Herzberg, G. *Infrared and Raman Spectra of Polyatomic Molecules*, First Edition.; D. Van Nostrand Company, 1945.

(4) Markovits, A.; García-Hernández, M.; Ricart, J. M.; Illas, F. Theoretical Study of Bonding of Carbon Trioxide and Carbonate on Pt(111): Relevance to the Interpretation of "in Situ" Vibrational Spectroscopy. *J. Phys. Chem. B* **1999**, *103* (3), 509–518. https://doi.org/10.1021/jp984016b.

(5) Iwasita, T.; Rodes, A.; Pastor, E. Vibrational Spectroscopy of Carbonate Adsorbed on Pt(111) and Pt(110) Single-Crystal Electrodes. *Journal of Electroanalytical Chemistry* **1995**, *383* (1), 181–189. https://doi.org/10.1016/0022-0728(94)03708-B.

(6) Berná, A.; Rodes, A.; Feliu, J. M.; Illas, F.; Gil, A.; Clotet, A.; Ricart, J. M. Structural and Spectroelectrochemical Study of Carbonate and Bicarbonate Adsorbed on Pt(111) and Pd/Pt(111) Electrodes. *J. Phys. Chem. B* **2004**, *108* (46), 17928–17939. https://doi.org/10.1021/jp048082r.

(7) Wan, E.; Travert, A.; Quignard, F.; Tichit, D.; Tanchoux, N.; Petitjean, H. Modulating Properties of Pure ZrO2 for Structure–Activity Relationships in Acid-Base Catalysis: Contribution of the Alginate Preparation Route. *ChemCatChem* **2017**, *9* (12), 2358–2365. https://doi.org/10.1002/cctc.201700171.

(8) Korhonen, S. T.; Calatayud, M.; Krause, A. O. I. Structure and Stability of Formates and Carbonates on Monoclinic Zirconia: A Combined Study by Density Functional Theory and Infrared Spectroscopy. *J. Phys. Chem. C* **2008**, *112* (41), 16096–16102. https://doi.org/10.1021/jp803353v.

(9) Andrews, M. A.; Gould, G. L.; Klooster, W. T.; Koenig, K. S.; Voss, E. J. Syntheses, Spectra, and Structures of (Diphosphine)Platinum(II) Carbonate Complexes. *Inorg. Chem.* **1996**, *35* (19), 5478–5483. https://doi.org/10.1021/ic9603159.